Atmos. Chem. Phys. Discuss., 13, 17021–17052, 2013
www.atmos-chem-phys-discuss.net/13/17021/2013/
doi:10.5194/acpd-13-17021-2013

Atmospheric Chemistry and Physics
Discussions
Open Access

Understanding atmospheric mercury speciation and mercury in snow over time at Alert, Canada

A. Steffen[1,2], J. Bottenheim[1], A. Cole[1], R. Ebinghaus[2,3], G. Lawson[4], and W. R. Leaitch[1]

[1]Air Quality Processes Research Section, Environment Canada, 4905 Dufferin St., Toronto, Ontario, Canada, M3H 5T4
[2]Leuphana University Lüneburg, Institute of Sustainable & Environmental Chemistry (ISEC), Scharnhorststr. 1/13,21335 Lüneburg
[3]Helmholtz-Zentrum Geesthacht, Institute of Coastal Research, Department for Environmental Chemistry, Max-Planck-Str. 1, 21502 Geesthacht
[4]Environment Canada, Science and Technology Branch, 867 Lakeshore Rd, Burlington, Ontario, L7R 4A6

Received: 29 May 2013 – Accepted: 10 June 2013 – Published: 26 June 2013

Correspondence to: A. Steffen (alexandra.steffen@ec.gc.ca)

Published by Copernicus Publications on behalf of the European Geosciences Union.

Abstract

Ten years of atmospheric mercury speciation data and 14 yr of mercury in snow data from Alert, Nunavut, Canada are examined. The speciation data, collected from 2002 to 2011, includes gaseous elemental mercury (GEM), particulate mercury (PHg) and reactive gaseous mercury (RGM). During the winter-spring period of atmospheric mercury depletion events (AMDEs), when GEM is close to being completely depleted from the air, the concentrations of PHg and RGM rise significantly. During this period, the median concentrations for PHg is 28.2 pg $m^{-3}$and RGM is 23.9 pg m^{-3} from March to June in comparison to the annual median concentrations of 11.3 and 3.2 pg m^{-3} for PHg and RGM, respectively. In each of the ten years of sampling, PHg increases steadily from January through March and is higher than RGM. This pattern begins to change in April with very high levels of PHg and increasing RGM. In May, RGM transitions to be significantly higher than PHg and continues into June whereas PHg sharply drops down. The transition is thought to be driven by a combination of air temperature and particle availability. Firstly, the ratio of PHg to RGM is favoured by low temperatures suggesting that oxidized mercury may partition to available particles to form PHg. Prior to the transition, the median air temperature is −24.8 °C and after the transition the median air temperature is −5.8 °C. Secondly, high aerosol levels in the spring are a strong driver for the high PHg concentrations. In February through April, partitioning of oxidized mercury to produce PHg was favoured by increased concentrations of particles that are principally the result of Arctic Haze and some sea salts. In the snow, the concentrations of mercury peak in May for all years. The highest deposition of mercury to the snow in the spring at Alert is during and after the transition of PHg to RGM in the atmosphere.

1 Introduction

Mercury has created quite a stir in the high Arctic air over the past two decades because of its interesting springtime atmospheric chemistry and its impact on the environment. Since there are virtually no local sources of mercury in the Arctic, its presence is thought to be due to long range transport from Asia, Russia, North America and Europe (Durnford et al., 2010). The atmospheric processes that dominate the springtime oxidation and deposition of mercury can drive some of this long range transported mercury onto the Arctic surface. It has been demonstrated that, during the polar spring, gaseous elemental mercury (GEM) oxidizes to shorter lived mercury species known as reactive gaseous mercury (RGM) (Schroeder et al., 1998; Lindberg et al., 2001). RGM can either be in the air as a gas or adsorbed to particles and be reported as particulate mercury (PHg). Many studies have reported the decrease in GEM and a coincidental increase in speciated mercury (PHg and RGM) and the association of this chemistry with spring time ozone and halogen chemistry (Lindberg et al., 2001; Lindberg et al., 2002; Aspmo et al., 2005; Kirk et al., 2006; Cobbett et al., 2007; Dastoor et al., 2008; Steffen et al., 2008; Steen et al., 2011). There are few long term data sets of speciated atmospheric mercury that have looked at processes in the high Arctic, with the exception of Cole et al. (2013) who reported on the long term trends at Alert.

Alert is a high Arctic site, located at the tip of Ellesmere Island, Nunavut, Canada. Long term atmospheric measurements of GEM have been undertaken since 1995 (Schroeder et al., 1998; Cole and Steffen, 2010) and speciation data have been collected since 2002. The unique GEM annual signature from Alert has been previously published (Schroeder et al., 1998; Steffen et al., 2005; Cobbett et al., 2007; Cole and Steffen, 2010) showing northern hemispheric background levels in the fall and winter, low concentrations in the spring and higher concentrations in the summer. The lifetime of atmospheric mercury depends on its chemical form and is considered to be GEM $\gg$ PHg $>$ RGM (Schroeder and Munthe, 1998). The dry deposition velocities of these species have been modeled to be RGM $>$ PHg $>$ GEM (Zhang et al., 2009). The fractionation of these Hg species depends on location and chemistry with GEM being the predominant species in the air in most locations (generally the sum of all Hg species consists of 98 % GEM, 1.5 % RGM and 0.5 % PHg, Peterson et al., 2009). However, at locations in the Arctic (and Antarctic) this fractionation changes during the spring months; at Alert for example, to 88.5 % GEM, 4.5 % RGM and 7 % PHg (from 2002 to 2011 using mean concentrations) or 95.6 % GEM, 2 % RGM and 2.4 % PHg (using median concentrations). It is well known that a series of photochemically initiated reactions can oxidize GEM to an Hg^{2+} inorganic species (Simpson et al., 2007; Ariya et al., 2008; Obrist et al., 2011) either in the gas phase (as RGM) or associated to particles (as PHg). These reactions result in atmospheric mercury depletion events (AMDEs) and refer to the depletion of GEM from the troposphere. This loss has been explained as conversion of GEM to other mercury species and/or a loss to the snow surface (Steffen and Cole, 2008).

Currently, the actual chemical identity of RGM and PHg are not well determined, they are operationally defined as the fraction of gaseous mercury that can be separated from the air by a KCl coated denuder and mercury associated with particles collected on a quartz filter, respectively (Sheu and Mason, 2004; Gustin and Jaffe, 2010). Analysis methods for RGM and PHg include separation of the species and quantification as GEM. While there are reasonably reliable reference standards for GEM (Temme et al., 2007), there exist none to accurately quantify and elucidate RGM and PHg (Temme et al., 2007; Gustin and Jaffe, 2010). The data set used for the current study was obtained using sampling protocols, quality control and analysis as described by Steffen et al. (2012). The data were collected over a 10 yr period were compared from year to year to observe recurring patterns and potential processes.

Aerosol particles have been studied at Alert since 1980 (Barrie, 1986; Barrie et al., 1989; Gong et al., 1997; Sirois and Barrie, 1999; Sharma et al., 2004). The well known phenomenon of Arctic Haze is due to air masses originating from anthropogenic emissions in Europe, North America and the former Soviet Union, that are transported to and trapped in the Arctic air. The haze primarily consists of sulphate and carbonaceous particles, maximizing in March and April (Sharma et al., 2004; Quinn et al., 2007).

This study reports an analysis of ten years of mercury sampling in air and fourteen years of mercury sampling of the snow coupled with atmospheric meteorological and particle measurements from Alert.

2 Methods

2.1 Sample location

Alert, Nunavut, Canada is located at 82.5° N and 62.3° W, 800 km from the geographic North Pole. The instrumentation is located at the Dr. Neil Trivett Global Atmospheric Watch (GAW) Observatory on the north eastern edge of Ellesmere Island. The laboratory is located approximately 8 km from the shore of the Lincoln Sea and is at an elevation of 195 m a.s.l. The atmospheric mercury speciation and particulate instruments are located on an outside walk up tower approximately three and five metres above the ground, respectively. The tables from which the snow samples were collected are located approximately 200 m south of the laboratory.

2.2 Atmospheric mercury speciation

GEM, PHg and RGM were collected using the Tekran 2537A/1130/1135 automated mercury vapour analyzer system. The methods have been described in detail elsewhere (Landis et al., 2002; Steffen and Cole, 2008). In short: air is pulled into the analyzer through a Teflon® coated elutriator and impactor designed to remove particles and snow $> 2.5\,\mu m$ at flow rates of $10.0\,L\,min^{-1}$ (particle size cut off varies with flow rate). The sample air flows via a KCl coated quartz denuder to trap RGM in the 1130 unit, and then passes over a quartz particulate filter to trap PHg in the 1135 unit. GEM passes through both the 1130 and 1135 units and is carried into the 2537 analyzer (at a flow rate of 1 L min^{-1}) for analysis. GEM is reported as ng m^{-3} of mercury. The samples are analysed by first heating an inline pyrolyzer to 800 °C. The quartz filter is then heated to desorb the PHg and sent through the pyrolyzer to break all PHg to GEM which is then analysed by the 2537A instrument. The denuder is then heated to 600 °C to release the RGM and passes over the pyrolyzer to break down all RGM to GEM which is analysed by the 2537A instrument. PHg and RGM are reported as pg m^{-3} of mercury. Mercury free zero air is passed through the system before and after these desorption cycles as blanks. At Alert, air samples were originally collected for 3 h to ensure there was enough mercury collected for analysis and once verified the sampling time was reduced to 2 h. Rigorous procedures during and after sample collection/analysis have been established for Alert to ensure consistency from year to year and are described in detail in Steffen et al. (2012).

The analytical detection limits of the Tekran® 2537 analyzer (< 0.1 ng m^{-3}, from the manufacturer, or 0.75 pg of mercury collected based on a 7.5 L sample volume) are more than an order of magnitude below ambient GEM concentrations (typically > 1 ng m^{-3}). For the PHg and RGM data collected at Alert, the detection limits are calculated to be three times the standard deviation of the two post desorption blanks. The detection limits for PHg and RGM at Alert for each year from 2002 to 2011 are shown in Table 1.

2.3 Meteorological data

The air temperature is measured at the GAW station at a 1 Hz frequency using a Campbell 107F thermistor (USA). Prior to 2004, relative humidity (RH) is calculated from the dew point measured with a custom Atmospheric Environmental Services Type E dew cell (AES Drawing series 0306) at the Alert station (station #2400300, 82°31′4″ N, 62°16′50″ W, 30.48 m). All RH measurements after 2004/06/26 are from a Vaisala RH sensor (model HMP45C212) at the Alert Climate station (2400305, 82°30′ N, 62°20′ W, 65.4 m). Data are obtained from the Environment Canada National Climate Data and Information Archive (http://climate.weatheroffice.gc.ca/contacts/index_e.html).

2.4 Aerosol particle volume and light scattering

The ambient aerosol is pulled into the laboratory through a 3 m long, 10 cm diameter stainless steel vertical manifold at a flow rate of about 1000 L min^{-1}. Particles are sampled out of the manifold from near the center of the flow stream, about 30 cm up from the bottom of the manifold. From there the particles are delivered to the sampling devices via stainless steel tubing. The mean total residence time of a particle from outside to its measurement point is approximately 3 s and, at this point, the particle at approximately room temperature and the relative humidity (RH) is < 50 %. Particle size distributions from 20 nm to 500 nm are measured with a TSI 3034 Scanning Mobility Particle System (SMPS) which is calibrated on site using monodisperse particles of polystyrene latex and of ammonium sulphate generated with a Brechtel Manufacturing Incorporated (BMI) Scanning Electrical Mobility Spectrometer (SEMS). Particle volume concentrations in the size range of 20 nm to 500 nm are derived from the integration of the SMPS size distribution assuming spherical particles.

Particle volume dry scattering coefficients (σ_{sp}) in < 1 and < 10 µm sizes are measured by a 3-λ Integrating Nephelometer (TSI Model 3563). The instrument is calibrated by using high purity dry CO_2 and drift in the calibration is checked weekly. Measurement uncertainties of the TSI nephelometer have been described in detail elsewhere (Anderson and Ogren, 1998; Anderson et al., 1999; Sheridan et al., 2002). The nephelometer data used in this paper are particle light scattering coefficients (b_{sca}) at 550 nm wavelength and represents particles greater than 500 nm in diameter (from 2004–2006 there was no size selection so all particles were collected, post 2006 a 10 µm cut-off was employed).

2.5 Snow sampling

One litre wide-mouth glass jars are used for sample collection. PTFE lined polypropylene (PP) lids were used until 2001 and then replaced with solid PFA Teflon lids (Savillex). The snow is collected on tables and the ground located behind the GAW lab. Snow samples are collected on a snow event basis when the local operator is available to collect the sample. There are two tables approximately 1 m × 1 m each from which the samples are collected. The tables are made of a wooden platform covered with a 1/32″ thick PTFE sheet that is attached to the table surrounded by a 1″ × 1″ PTFE edge. The platform is mounted on Dexion steel strips and the legs are dug into the tundra for stability. When there is a layer of snow on the tables, three bottles of snow are collected using gloved hands, a PTFE scraper and a scoop made from a PTFE bottle. The snow is collected into a pile with the scraper and scooped into glass jars from the snow tables. The tables are divided into three sections and each area of sample collected is measured. When the samples have been collected, the remainder of snow is scraped off so that the table is left blank and ready to collect the next snowfall. Using a very similar procedure, ground samples are collected close to the tables. The surface snow (approximately 1 cm deep) is scraped into a pile using a Teflon scraper. The snow is then scooped into the glass sample jars. Snow samples are kept in the jars in sealed zip locked bags, in coolers and are kept frozen. The coolers are filled with snow and hand carried from Alert to Toronto where they remain frozen until analysis.

2.6 Snow analysis

The sample jars and lids are cleaned in a multi-stage process: soap bath, concentrated hydrochloric acid, concentrated nitric acid, then air dried in a clean-lab. Jars are numbered and pre-weighed before they are packed in coolers and sent to Alert. Blank water is generated using a multi-stage purification process: reverse osmosis, distillation, passage through two Milli-Q systems with UV-digestion. Bromine monochloride (0.1 N BrCl) is prepared using low-Hg hydrochloric acid (HCl; JT Baker Instraanalyzed), bromic acid (Sigma) and potassium bromate (Alfa Aesar). Alkaline stannous sulphate is produced from stannous sulphate (Alfa Aesar and Sigma) and low-Hg sodium hydroxide (Anachemia Science).

Prior to analysis, sample jars are weighed and 0.1N BrCl is added to the thawing snow samples to give a final concentration of 0.4 %. Total-Hg in the melted snow is determined by direct cold-vapor atomic fluorescence detection after reduction with alkaline stannous sulphate. The detection limits of this method are typically 0.05 pg $\mathrm{mL^{-1}}$, based on three times standard deviation of the analytical blanks. The analytical system couples an autosampler (Gilson 222) and an atomic fluorescence detector (Tekran 2500) and uses a chromatography interface and software for signal capture and peak integrations. The phase separator was built in-house and made of PFA Teflon with a polyethylene gas bubbler and actively pumped liquid inlet and outlets. A gas phase drier (Nafion) removes water from the sample gas before it passes into the AFS detector.

Quality assurance and control samples included laboratory, bottle, trip and field blanks. In all cases, 250 mL of ultra-pure blank water is added to the blank jars, along with 0.1 N BrCl to give the same concentration as the samples. The 250 mL value is selected because it was close to the average volume of the melted snow samples. Standard reference water is run alongside samples during analyses. All samples are pre-screened by running 10 mL single samples to determine general THg concentrations. The samples are split into low and high samples to fit calibration standards with equivalent concentration ranges. The final analytical runs determined samples as duplicates or triplicates and spike recoveries were determined every eight to ten samples. Analytical blank results are not subtracted from sample results, since the blank water is independent of the sample results and reagents used have been determined to be below the detection limits of the method. These blank results are used as a base value for the various other blanks determined. Field blank averages are used to correct sample results, after conversions to average mass per jar values.

3 Results and discussion

3.1 Long-term speciation data

Ten years of gaseous elemental mercury (GEM), reactive gas phase mercury (RGM) and particulate mercury (PHg) concentration measurements from Alert, Canada from 2002 to 2011 are shown in Fig. 1. Measuring accurate and reliable atmospheric GEM, RGM and PHg has its challenges (Gustin and Jaffe, 2010) especially in the remote high Arctic. Few long term mercury speciation measurements have been reported around temperate regions and only one for the Arctic (Cole et al., 2013). This time series shows that the annual signature of mercury species repeats from year to year. The years 2003, 2006 and 2010 are not anomalous but reflect instrumental problems and hence a lack complete data sets for those years.

Figure 2 shows box plots of the monthly concentrations of GEM, RGM and PHg over the 10 yr period. The middle line in the box indicates the median concentration; the bottom and top of the box represent the 25th and 75th percentiles; the whiskers above and below the box indicate the 90th and 10th percentiles and the dots indicate the maximum and minimum values in the data set. A distinct annual cycle for all three species is highlighted in this figure. Annual statistics of PHg and RGM show considerable variability among years. The monthly and overall statistics of PHg and RGM are presented in Table 2. The overall PHg and RGM median concentrations for the 10 yr period are 11.3 and 3.2 $\mathrm{pg\,m^{-3}}$, respectively, but as is clear from Fig. 2, there are considerable changes in the concentrations throughout the year. PHg is very low in the months June through October (median $< 8.4\,\mathrm{pg\,m^{-3}}$) but begins to increase in November through February (median range $\sim$ 9–42 $\mathrm{pg\,m^{-3}}$). This pattern is seen each year and is not considered anomalous. High variability in all the data is observed from March to May and the springtime chemistry is evident in the elevated March to May PHg levels (median range 21–103 $\mathrm{pg\,m^{-3}}$). The increase in PHg over the winter is not considered to be reflective of AMDE chemistry but may be a product of transport association with winter particle pollution (Arctic haze). In contrast, RGM is very low from

August to February (median range 0.7–5.3 pg m^{-3}), slightly elevated in March and July (median 7.4 and 4.6 pg m^{-3}, respectively) and high April to June (median range 17–100 pg m^{-3}). It has been reported that AMDEs stop when the temperature is sustained above 0 °C (Steffen et al., 2005), however there appears to be production of RGM well into July where air temperatures are above 0 °C. This annually occurring higher level of RGM in July is variable in concentration and unexpected but is not considered to be a result from AMDE chemistry. This study focuses on the springtime chemistry from March to June inclusive. Further in depth investigations into the annual cycling of PHg and RGM at Alert must be undertaken to explain these patterns.

Finally, Fig. 2 shows the clear decrease in GEM in March concurrent with a notable increase in PHg followed by an increase in RGM in May. PHg reaches its maximum in April and then trails off. In May, the RGM concentrations are highest and trail off into June where GEM concentrations begin to increase again. Cobbett et al. (2007), reported a transition of PHg to RGM in the spring of 2005 at Alert and we report here that this transition occurs each year around the same time (within a 2 week period) for the ten years of measurements. This transition from PHg to RGM was also observed in 2004 in Churchill, Canada on Hudson's Bay around the same time of the year (Kirk et al., 2006) and over a longer period at Ny-Alesund in 2007/08 (Steen et al., 2011).

3.2 Factors affecting the transition from PHg to RGM

Previous field and modeling studies have suggested that factors such as specific humidity, air temperature, wind speed and aerosol particle loadings impact the fractionation of mercury species (Cobbett et al., 2007; Rutter and Schauer, 2007a,b; Amos et al., 2012). Here relative humidity (RH), air temperature and particle concentration are investigated for their possible roles in the fractionation of mercury species at Alert. Monthly plots of air temperature (top) and RH (bottom) for years 2002–2011 and 2004–2011, respectively, are shown in Fig. 3. The median RH increases substantially from April to May. Before the PHg to RGM transition, the April median RH is 74 % and after the transition the May RH is 85 %. It has been suggested that a threshold of 75 % RH marks a decrease in the PHg concentrations in the Arctic spring (Steffen et al., 2013). Since RH is temperature dependant and describes the water content relative to saturation, absolute water content (AWC) is also plotted (middle). In Fig. 3, both RH and AWC follow the same pattern with temperature throughout the year and a similar steep increase in both parameters is shown March to May. It can be conceivable that the transition of PHg to RGM from April to May could be related to water absorption by aerosols. However, we suggest that other factors affect the transition of PHg to RGM more effectively and are described below.

The dependence of the transition on the air temperature was investigated by looking at the fraction of PHg relative to [PHg] + [RGM] or Hg(f) (f indicates fraction). Regressions of Hg(f) versus temperature (Fig. 4) indicate that a higher Hg(f) is associated with colder temperatures. The linear regression r^2 values and line slopes for each year from February to June are shown in Fig. 4. For this part of the study, data from the years 2003, 2006, 2007 and 2010 were not included because of large data gaps. The relationships in Fig. 4 are in keeping with the findings of Rutter and Schauer (2007b) who reported a linear relationship between the logarithm of inverse gas to particle partitioning and inverse air and were later confirmed by Amos et al. (2012). The former study's data was limited to a minimum air temperature of −3 °C and the latter used temperatures down to −16.7 °C. Our study reflects a temperature range of −40 to +20 °C. Our data cannot be directly compared with these two studies, as there are no $PM_{2.5}$ data available from Alert to calculate the particle surface area so that the PHg data can be normalized over differently sized particle surfaces. However, the slopes of the linear regressions between years are very close (see Fig. 4) indicating the relationship between the air temperature and Hg(f) is similar each year. The years where this relationship is not reasonably significant between air temperature and PHg are 2005 and 2008 which shows a high Hg(f) at temperatures between −5 and 5 °C due to anomalously high PHg concentrations. We have no explanation for the elevated PHg at these times. Cole and Steffen (Cole and Steffen, 2010) reported a relationship between air temperature and the frequency of depletion events. They reported that there were higher frequencies of depleted GEM reported in March when temperatures were between −40 and −45 °C and between −25 and −20 °C in May and suggested that the latter temperature may be related to the initiation of bromine chemistry but did not provide a firm explanation for this relationship. Before the transition (March to April), when Hg(f) is greater than 0.5 (predominantly PHg), the median air temperature is −24.8 °C and after the transition, when Hg(f) is less than 0.5 (predominantly RGM), the median air temperature is −5.8 °C. Thus, results from this study show that PHg is predominant at lower temperatures and suggests that the lower temperatures drive the partitioning of oxidized mercury from RGM towards PHg. Further, the average temperature during the week of transition for all the years, except 2003 and 2010, is −15.6 ± 2.8 °C. Indeed, modelling studies have predicted that in colder air masses the predominant Hg^{+2} fraction will be PHg rather than RGM (Amos et al., 2012). We conclude that temperature is a significant driver in the transition of PHg to RGM at Alert during the spring.

The potential impact of the atmospheric aerosol loading on the speciation transition from PHg to RGM is also considered. The aerosol is represented here in two ways: (1) using the particle light scattering measurements from the nephelometer, which is approximately proportional to the surface area of the submicron aerosol, and (2) the volume concentration of the sub-500 nm diameter particles, which is proportional to the mass concentration of the aerosol. The light scattering data are available back to 2004, whereas the volume concentration data are only available since 2011; for the long-lived aerosol measured at Alert, these two quantities are also proportional to each other. Figure 5 shows monthly box and whisker plots of the particle light scattering coefficient (b_{sca}) at 550 nm wavelength (yellow boxes) and Hg(f) (grey boxes) for January to June. From January to April both b_{sca} and Hg(f) are relatively steady. In May, when the transition from pHg to RGM occurs, Hg(f) decreases to lower values concurrent with a significant decrease in the b_{sca}. The slight increase in the PHg fraction in June is curious and may reflect the relatively low PHg and RGM concentrations in comparison to the high values in the previous months (Table 2) and thereby skewing the Hg(f). Figure 6 shows PHg as a function of the total volume concentration of particles less than 500 nm for hourly averages during March through June 2011. These results show that PHg is associated with higher particle volume for March and April, May is a transition month to lower particle volume and June shows no association with PHg. That result is consistent with the trend of b_{sca} and Hg(f) in Fig. 5, indicating that a larger Hg(f) is associated with higher concentrations of particle surface area and volume. Since PHg is believed to be due to RGM adherence to particles in the air (Sheu and Mason, 2004) it is concievable that the presence of more particle surface area or volume in the air may contribute to an increased shift of RGM to PHg during January to April at Alert. The higher particle volume concentrations during January to April are linked with Arctic Haze (Barrie, 1986) and we hypothesize that the presence of Arctic haze is a significant contributor to the increased levels of PHg during this period. This is not the first report of an influence of arctic haze on mercury as Douglas and Sturm (2004) linked mercury levels and arctic haze in the snow around northern Alaska. Other aerosols such as sea salts and ice crystals are also common during the spring at Alert. Both these aerosols are effective scavengers of RGM and have been associated with elevated levels of PHg and Hg in the snow (Rutter and Schauer, 2007a; Douglas et al., 2008; Malcolm et al., 2010; Steffen et al., 2013). Coarse particle Na^+, mostly sea salt derived, is elevated in February and the beginning of March at Alert (Leaitch et al., 2013) but drops off in April while the PHg levels remain high; ice crystals were not measured at Alert. Partitioning of gas-phase mercury to particles can be dependent on the composition of the aerosol (Rutter and Schauer, 2007a). Particles containing sodium nitrate and sea salt components have shown the highest partition coefficients. Each year PHg at Alert begins to increase in March and then climbs to a maximum in April and are concurrent with sea salts and arctic haze particle increases. Further study is required to identify which types of particles dominate both the atmospheric transition and deposition of mercury in the spring.

3.2.1 Mercury in snow at Alert

Mercury can be deposited onto the snow and ice surfaces enabling its distribution into the environment. All 3 forms of mercury can deposit from the atmosphere to the snow surface. While RGM and PHg have higher deposition velocities than GEM, GEM deposition is significant because of its much higher concentration in the atmosphere compared to the other mercury species (Lin, 2006). However, for this paper, we are focussing on the deposition of RGM and PHg in the context of AMDE occurrence at Alert. A review of mercury behaviour in snow concluded that PHg deposited to snow is likely to remain in the snow pack, while deposited GEM is immediately re-emitted (Durnford and Dastoor, 2011). RGM undergoes several processes including photo reduction and emission and oxidation in the snow and thus its fate is uncertain (Durnford and Dastoor, 2011). These authors conclude that, because of the heterogeneity of snow and mercury deposition around the Arctic, single field studies reporting concentration of mercury in the snow may not allow for extrapolation of deposition on a regional scale.

Since 1998, snow samples have been collected at Alert in the spring just after a snow event. The number of samples has depended on the number of snow events occurring in a given year and on local operator availability to sample the snow. Figure 7 shows box and whisker plots of the concentrations of Hg from Alert (1998–2011) in the snow (in $\mathrm{pg\,g^{-1}}$) from both the table (top) and ground samples (bottom). It is evident that significantly lower Hg concentrations are observed from the ground samples in comparison to the table samples, reinforcing the use of snow table sampling here. Snow sampling was undertaken to investigate springtime chemistry and thus occurred only during the months of February to June. To the authors' knowledge, this is the only data set of its kind from the Arctic. Collecting snow on a table in this manner is believed to give a reasonable measure of Hg that is removed from the atmosphere by snow. Surface samples are generally collected from the first 1 cm of the snow pack but accurately limiting the sampling to that level is challenging and in any case may well contain some older snow which would bias the obtained concentrations of its components. Further-more, surface/ground snow samples can be compromised by contribution from blowing snow, multiple snow events and loss of deposited material to deeper layers of the snow pack.

Figure 7 shows the monthly distribution of Hg in snow from February to June from 1998 to 2011. These results show that there is a small but increasing amount of Hg in the snow in February, March and April and that levels peak in May and then trail off in June. There have been reports of similar observations from short term field studies or shorter times (Lu et al., 2001; Durnford and Dastoor, 2011) but nothing this extensive over such a long period of time.

The relationship between the level of Hg in the snow and the atmosphere (RGM and PHg) is explored in Fig. 8. We do not include GEM in this discussion because as mentioned earlier it is believed to be rapidly re-emitted from the snow. In this figure the mercury concentration in snow (2002–2011) is plotted together with PHg and RGM concentrations from February to June (averaged for each Julian day for all data from 2002 to 2011). It can be seen that when the PHg to RGM transition occurs in the atmosphere, there is an increase in Hg levels in the snow. This was found to repeat each year without fail, when snow samples were collected, over the ten-year period. We conclude that the highest deposition of mercury to the snow in the Arctic depends on what form of mercury is present in the atmosphere and the atmospheric conditions that lead to the presence of a given mercury fraction in the air. PHg is scavenged more efficiently by snow than RGM (Amos et al., 2012) which will aid in the deposition of PHg to the snow surface. As shown in Fig. 8, the decrease in PHg and drop in particle numbers in May coincides with the initial increase of Hg in the snow. Subsequently, the levels of mercury in snow keep rising (and falling) concurrently with the concentration of RGM. RGM is known to have a higher dry deposition velocity (Zhang et al., 2009) and can readily deposit onto the snow surfaces which could explain these trends. In any case, our data show that the highest deposition to the snow in the spring at Alert is during and after the transition of PHg to RGM in the atmosphere.

4 Conclusions

Atmospheric speciated mercury measurements reveal strong seasonality as well as significant variability within the spring season. Low PHg concentrations are found in the summer, increase towards the winter and peak in March and April. RGM concentration levels are lowest from August to February, peak in May and remain elevated until July. The most significant finding is the abrupt transition of PHg to RGM during April to May that is repeated over a ten-year period. Fourteen years of snow sampling data from Alert show that the concentrations of mercury in the snow increase as the spring season progresses, peak in May and decrease thereafter.

The results from considering atmospheric factors that may have an impact on the transition from PHg to RGM are as follows:

1. The partitioning of oxidized mercury shows a higher fraction of PHg at low temperatures. We hypothesize that this is due to increases partitioning of RGM to available particles at low temperatures. Prior to the transition from predominance of PHg, the median air temperature is –24.8 °C and after the transition the median air temperature is –5.8 °C. The average temperature over the transition period is $-15.6 \pm 2.8\,^{\circ}\mathrm{C}$.
2. The availability of high levels of aerosols during the springtime is a strong driver for the high PHg concentrations repeatedly reported during the Alert springtime period. From February to April particles such as arctic haze and sea salts can provide the surface area for RGM adsorption. A strong decrease in the particle concentration in the air is concurrent with a sharp decline in PHg.
3. It is possible that the transition of PHg to RGM from April to May could be related to water absorption by aerosols. However, we suggest that other factors affect the transition of PHg to RGM more effectively and are described below.

We believe that the transition in mercury speciation between particle phase and gas phase is primarily due to a combination of air temperature and particle concentration.

More investigation is needed to determine the relative roles of air temperature and particle concentration and to understand if particle-bound water is a significant factor in this transition. Fourteen years of snow sampling at Alert show that the concentrations of mercury in the snow increase as the spring season progresses, peak in May and decrease thereafter. Ten years of data from the snow and atmospheric measurements are linked to show that during the PHg transition to RGM there is a concurrent increase in the concentration of mercury in the snow; subsequent to this transition, the concentration in snow appears to mirror the rise and fall in the concentration of RGM in the air. Thus, the highest deposition of mercury to the snow in the spring at Alert is during and after the transition of PHg to RGM in the atmosphere.

Acknowledgements. Over 14 yr of data represents the work of many people and not only the authors. The authors wish to thank Arctic coordinator Andrew Platt and the many operators and students working in the Neil Trivett GAW laboratory at Alert during this time for maintaining the instruments and collecting all the samples, and Patrick Lee and John Deary for excellent technical support over the years. Special thanks to Christophe Ferrari and Christina Scherz whose preliminary work on this data put this ship on the right path; to Julie Narayan whose constant help with data is invaluable and to Greg Skelton for the QC development and implementation. Thanks to Sangeeta Sharma for the nephelometer data and Andrew Platt for the meteorological data. The Air Quality Research Division and the Climate Research Division of Environment Canada and Aboriginal Affairs and Northern Development Canada, Northern Contaminants Program are acknowledged for their long term commitment and financial support to this program. Finally, thanks to the Arctic Monitoring and Assessment Programme for their long term interest and support of this research.

References

Amos, H. M., Jacob, D. J., Holmes, C. D., Fisher, J. A., Wang, Q., Yantosca, R. M., Corbitt, E. S., Galarneau, E., Rutter, A. P., Gustin, M. S., Steffen, A., Schauer, J. J., Graydon, J. A., Louis, V. L. St., Talbot, R. W., Edgerton, E. S., Zhang, Y., and Sunderland, E. M.: Gas-particle partitioning of atmospheric Hg(II) and its effect on global mercury deposition, Atmos. Chem. Phys., 12, 591–603, doi:10.5194/acp-12-591-2012, 2012.

Ariya, P., Skov, H., Grage, M. M.-L., and Goodsite, M. E.: Gaseous elemental mercury in the ambient atmosphere: Review of the application of theoretical calculations and experimental studies for determination of reaction coefficients and mechanisms with halogens and other reactants, Adv. Quant. Chem., 55, 43–55, doi:10.1016/S0065-3276(07)00204-3, 2008.

Aspmo, K., Gauchard, P.-A., Steffen, A., Temme, C., Berg, T., Bahlmann, E., Banic, C., Dommergue, A., Ebinghaus, R., Ferrari, C., Pirrone, N., Sprovieri, F., and Wibetoe, G.: Measurements of atmospheric mercury species during an international study of mercury depletion events at Ny-Alesund, Svalbard, spring 2003. How reproducible are our present methods?, Atmos. Environ., 39, 7607–7619, 2005.

Barrie, L. A.: Arctic air pollution: An overview of current knowledge, Atmos. Environ., 20, 643–663, 1986.

Barrie, L. A., Olson, M. P., and Oikawa, K. K.: The flux of anthropogenic sulphur into the arctic from mid-latitudes in 1979/80, Atmos. Environ., 23, 2505–2512, 1989.

Cobbett, F. D., Steffen, A., Lawson, G., and Van Heyst, B. J.: Gem fluxes and atmospheric mercury concentrations (gem, rgm and hgp) in the canadian arctic at Alert, Nunavut, Canada (February–June 2005), Atmos. Environ., 41, 6527–6543, 2007.

Cole, A. S. and Steffen, A.: Trends in long-term gaseous mercury observations in the Arctic and effects of temperature and other atmospheric conditions, Atmos. Chem. Phys., 10, 4661–4672, doi:10.5194/acp-10-4661-2010, 2010.

Cole, A. S., Steffen, A., Pfaffhuber, K. A., Berg, T., Pilote, M., Poissant, L., Tordon, R., and Hung, H.: Ten-year trends of atmospheric mercury in the high Arctic compared to Canadian sub-Arctic and mid-latitude sites, Atmos. Chem. Phys., 13, 1535–1545, doi:10.5194/acp-13-1535-2013, 2013.

Dastoor, A., Davignon, D., Theys, N., van Roozendael, M., Steffen, A., and Ariya, P.: Modeling dynamic exchange of gaseous elemental mercury at polar sunrise, Environ. Sci. Technol., 42, 5183–5188, 2008.

Douglas, T. A. and Sturm, M.: Arctic haze, mercury and the chemical composition of snow across western alaska, Atmos. Environ., 38, 805–820, 2004.

Douglas, T., Sturm, M., Simpson, W., Blum, J., Alvarez-Aviles, L., Keeler, G., Perovich, D., Biswas, A., and Johnson, K.: The influence of snow and ice crystal formation and accumulation on mercury deposition to the arctic, Environ. Sci. Technol., 42, 1542–1551, 2008.

Durnford, D. and Dastoor, A.: The behavior of mercury in The Cryosphere: A review of what we know from observations, J. Geophys. Res.-Atmos., 116, D06305, doi:10.1029/2010JD014809, 2011.

Durnford, D., Dastoor, A., Figueras-Nieto, D., and Ryjkov, A.: Long range transport of mercury to the Arctic and across Canada, Atmos. Chem. Phys., 10, 6063–6086, doi:10.5194/acp-10-6063-2010, 2010.

Gong, S. L., Barrie, L. A., Prospero, J. M., Savoie, D. L., Ayers, G. P., Blanchet, J.-P., and Spacek, L.: Modeling sea-salt aerosols in the atmosphere 2. Atmospheric concentrations and fluxes, J. Geophys. Res., 102, 3819–3830, 1997.

Gustin, M. and Jaffe, D.: Reducing uncertainty in measurement and understanding of mercury in the atmosphere, Environ. Sci. Technol., 44, 2222–2227, 2010.

Kirk, J. L., St. Louis, V. L., and Sharp, M. J.: Rapid reduction and reemission of mercury deposited into snow packs during atmospheric mercury depletion events at Churchill, Manitoba, Canada, Environ. Sci. Technol., 40, 7590–7596, 2006.

Landis, M., Stevens, R. K., Schaedlich, F., and Prestbo, E. M.: Development and characterization of an annular denuder methodology for the measurement of divalent inorganic reactive gaseous mercury in ambient air, Environ. Sci. Technol., 36, 3000–3009, 2002.

Leaitch, R., Sharma, S., Huang, L., Toom-Sauntry, D., Chivulescu, A., macDonald, A., Salzen, v., Pierce, J. R., Bertram, A. K., Schroder, J. C., Shanz, N. C., Chang, R. Y.-W., and Norman, A.-L.: Dimethyl sulfide control of the clean summertime arctic aerosol and cloud, Elementa: Science of the Anthropocene, submitted, 2013.

Lin, C. J.: Scientific uncertainties in atmospheric mercury models I: Model science evaluation, Atmos. Environ., 40, 2911–2928, 2006.

Lindberg, S. E., Brooks, S. B., Lin, C. J., Scott, K., Meyers, T., Chambers, L., Landis, M., and Stevens, R. K.: Formation of reactive gaseous mercury in the arctic: Evidence of oxidation of hg0 to gas-phase hg-ii compounds after arctic sunrise, Water Air Soil Pollut., 1, 295–302, 2001.

Lindberg, S. E., Brooks, S., Lin, C.-J., Scott, K. J., Landis, M. S., Stevens, R. K., Goodsite, M., and Richter, A.: Dynamic oxidation of gaseous mercury in the arctic troposphere at polar sunrise, Environ. Sci. Technol., 36, 1245–1256, 2002.

Malcolm, E. G., Ford, A. C., Redding, T. A., Richardson, M. C., Strain, B., and Tetzner, S. W.: Experimental investigation of the scavenging of gaseous mercury by sea salt aerosol, J. Atmos. Chem., 63, 221–234, doi:10.1007/s10874-010-9165-y, 2010.

Obrist, D., Tas, E., Peleg, M., Matveev, V., Fain, X., Asaf, D., and Luria, M.: Bromine-induced oxidation of mercury in the mid-latitude atmosphere, Nat. Geosci., 4, 22–26, 2011.

Peterson, C., Gustin, M., and Lyman, S.: Atmospheric mercury concentrations and speciated measured from 2004 to 2007 in reno, nevada, USA, Atmos. Environ., 43, 4646–4654, doi:10.1016/j.atmosenv.2009.04.053, 2009.

Quinn, P. K., Shaw, G. E., Andrews, E., Dutton, E. G., Ruhoh-Airola, T., and Gong, S.: Arctic haze: Current trends and knowledge gaps, Tellus B, 59, 99–111, doi:10.1111/j.1600-0889.2006.00238.x, 2007.

Rutter, A. P. and Schauer, J. J.: The impact of aerosol composition on the particle to gas partitioning of reactive mercury, Environ. Sci. Technol., 41, 3934–3939, 2007a.

Rutter, A. P. and Schauer, J. J.: The effect of temperature on the gas-particle partitioning of reactive mercury in atmospheric aerosols, Atmos. Environ., 41, 8647–8657, doi:10.1016/j.atmsoenv.2007.07.024, 2007b.

Schroeder, W. H. and Munthe, J.: Atmospheric mercury – an overview, Atmos. Environ., 32, 809–822, 1998.

Schroeder, W. H., Anlauf, K. G., Barrie, L. A., Lu, J. Y., Steffen, A., Schneeberger, D. R., and Berg, T.: Arctic springtime depletion of mercury, Nature, 394, 331–332, 1998.

Sharma, S., Lavoue, D., Cachier, H., Barrie, L. A., and Gong, S. L.: Long-term trends of the black carbon concentrations in the canadian arctic, J. Geophys. Res., 109, D15203, doi:10.1029/2003JD004331, 2004.

Sheu, G.-R., and Mason, R. P.: An examination of the oxidation of elemental mercury in the presence of halide surfaces, J. Atmos. Chem., 48, 107–130, 2004.

Simpson, W. R., von Glasow, R., Riedel, K., Anderson, P., Ariya, P., Bottenheim, J., Burrows, J., Carpenter, L. J., Frieß, U., Goodsite, M. E., Heard, D., Hutterli, M., Jacobi, H.-W., Kaleschke, L., Neff, B., Plane, J., Platt, U., Richter, A., Roscoe, H., Sander, R., Shepson, P., Sodeau, J., Steffen, A., Wagner, T., and Wolff, E.: Halogens and their role in polar boundary-layer ozone depletion, Atmos. Chem. Phys., 7, 4375–4418, doi:10.5194/acp-7-4375-2007, 2007.

Sirois, A. and Barrie, L. A.: Arctic lower troposheric aerosol trends and composition at alert, canada: 1980–1995, J. Geophys. Res., 104, 11599–11618, 1999.

Steen, A. O., Berg, T., Dastoor, A. P., Durnford, D. A., Engelsen, O., Hole, L. R., and Pfaffhuber, K. A.: Natural and anthropogenic atmospheric mercury in the European Arctic: a fractionation study, Atmos. Chem. Phys., 11, 6273–6284, doi:10.5194/acp-11-6273-2011, 2011.

Steffen, A. and Cole, A.: Mercury measurments at alert, Indian and Northern Affairs Canada, OttawaQS-8602-070-BB-A1, 182–188, 2008.

Steffen, A., Schroeder, W. H., Macdonald, R., Poissant, L., and Konoplev, A.: Mercury in the arctic atmosphere: An analysis of eight years of measurements of gem at Alert (Canada) and a comparison with observations at Amderma (Russia) and Kuujjuarapik (Canada), Sci. Total. Environ., 342, 185–198, 2005.

Steffen, A., Douglas, T., Amyot, M., Ariya, P., Aspmo, K., Berg, T., Bottenheim, J., Brooks, S., Cobbett, F., Dastoor, A., Dommergue, A., Ebinghaus, R., Ferrari, C., Gardfeldt, K., Goodsite, M. E., Lean, D., Poulain, A. J., Scherz, C., Skov, H., Sommar, J., and Temme, C.: A synthesis of atmospheric mercury depletion event chemistry in the atmosphere and snow, Atmos. Chem. Phys., 8, 1445–1482, doi:10.5194/acp-8-1445-2008, 2008.

Steffen, A., Scherz, T., Olson, M. L., Gay, D. A., and Blanchard, P.: A comparison of data quality control protocols for atmospheric mercury speciation measurements, J. Environ. Monitor., 14, 752–765, doi:10.1039/c2em10735j, 2012.

Khaykin, S. M., Pommereau, J.-P., and Hauchecorne, A.: Impact of land convection on the thermal structure of the lower stratosphere as inferred from COSMIC GPS radio occultations, Atmos. Chem. Phys. Discuss., 13, 1–31, doi:10.5194/acpd-13-1-2013, 2013.

Temme, C., Blanchard, P., Steffen, A., Beauchamp, S. T., Poissant, L., Tordon, R. J., and Weins, B.: Trend, seasonal and multivariate analysis study of total gaseous mercury data from the canadian atmospheric mercury measurement network (camnet), Atmos. Environ., 41, 5423–5441, 2007.

Zhang, L., Wright, L. P., and Blanchard, P.: A review of current knowledge concerning dry deposition of atmospheric mercury, Atmos. Environ., 43, 5853–5864, 2009.

Table 1. Detection limits for each year for annual and springtime measurements and the number of samples represented for each data point from 2002 to 2011 at Alert, Canada. Detection limits are reported in pg m^{-3}.

Detection Limit (pg m^{-3})	2002	2003	2004	2005	2006	2007	2008	2009	2010	2011
Annual	10.50	5.50	2.08	1.80	0.73	5.39	1.16	2.25	1.10	1.47
Spring	1.33	6.24	3.08	2.63	1.17	7.89	1.32	3.61	1.93	1.88
No. of samples										
Annual	1954	2169	3525	3130	5232	4220	4262	4482	3070	3711
Spring	864	533	916	1000	1452	834	1176	1262	498	1208

ACPD
13, 17021–17052, 2013

Title Page
Abstract | Introduction
Conclusions | References
Tables | Figures
◀| |▶
◀ ▶
Back | Close
Full Screen / Esc
Printer-friendly Version
Interactive Discussion

Table 2. Descriptive statistics of PHg (top) and RGM (bottom) for monthly data and overall data between 2002 and 2011 at Alert, Canada. All concentrations for mean, median, standard deviation (std dev) and maximum are reported in pg m^{-3}. Number represents the number of data points included in the statistics. Mean monthly air temperature is reported in °C.

PHg	Mean	Median	Std Dev	Maximum	Number	Air Temp
Jan	20.4	13.39	18.08	99.26	1023	−28.0
Feb	50.26	41.87	53.31	520.54	926	−30.3
Mar	136.67	102.60	110.38	541.51	1175	−30.5
Apr	149.58	80.56	154.48	748.69	1710	−22.8
May	45.46	21.15	71.74	698.03	1688	−10.6
Jun	12.76	8.40	15.45	153.33	1517	−0.18
Jul	7.36	4.66	7.10	40.98	1638	+4.3
Aug	6.22	3.38	9.55	85.76	1642	+2.2
Sep	5.30	4.54	5.39	48.26	924	−7.39
Oct	10.25	5.46	12.37	70.40	1194	−16.5
Nov	15.25	9.61	17.46	122.30	1297	−23.2
Dec	18.35	9.58	21.91	135.62	1349	−27.4
Overall	41.3	11.3	82.3	748.69	16 083	

RGM	Mean	Median	Std Dev	Maximum	Number
Jan	2.36	2.13	1.22	7.79	942
Feb	5.25	4.98	2.92	37.57	837
Mar	11.35	7.40	15.63	220.56	1147
Apr	33.96	22.20	35.78	331.87	1714
May	120.11	99.88	94.67	877.85	1630
Jun	41.09	16.76	62.13	718.02	1516
Jul	14.78	4.60	30.77	260.95	1687
Aug	4.35	1.46	8.75	108.82	1732
Sep	1.01	0.71	1.37	13.93	1069
Oct	0.88	0.70	0.90	7.99	1452
Nov	1.08	0.94	0.99	10.71	1451
Dec	1.86	1.71	1.98	20.72	1410
Overall	22.6	3.17	51.99	877.85	16 587

Note Minimum values for PHg ranged from 0 to 1.6 and for RGM 0 to 0.4

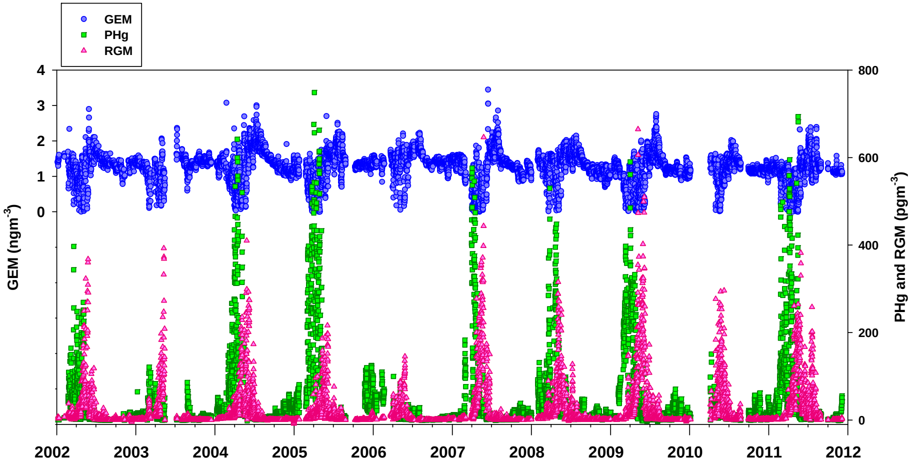

Fig. 1. Six hourly averaged data for gaseous elemental mercury (GEM – blue), particulate mercury (PHg-green) and reactive gaseous mercury (RGM – pink) from 2002 to 2011 at Alert Nunavut, Canada

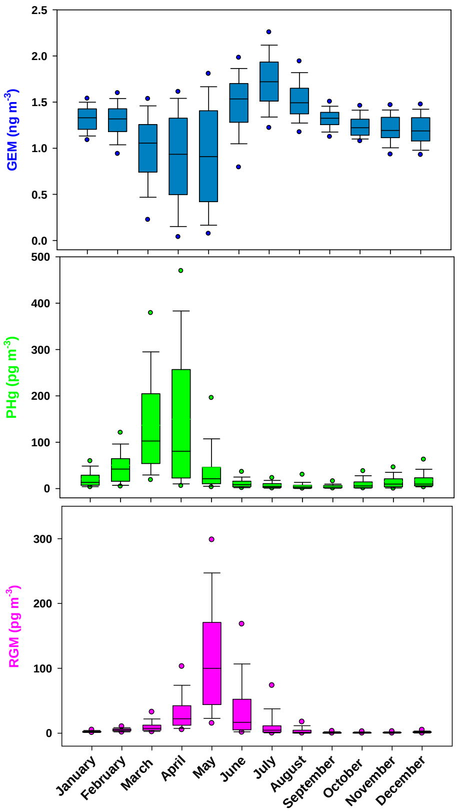

Fig. 2. Box and whisker plots of monthly gaseous elemental mercury (GEM – blue), particulate mercury (PHg – green) and reactive gaseous mercury (RGM – pink) from Alert, 2002–2011. GEM is in ng m^{-3} and PHg and RGM are in pg m^{-3}. Centre line in the box represents the median value, the boundaries of the box represent the 25th and 75th percentiles, the whiskers represent the 10th and 90th percentile and the dots represent the maximum and minimum values in the data set.

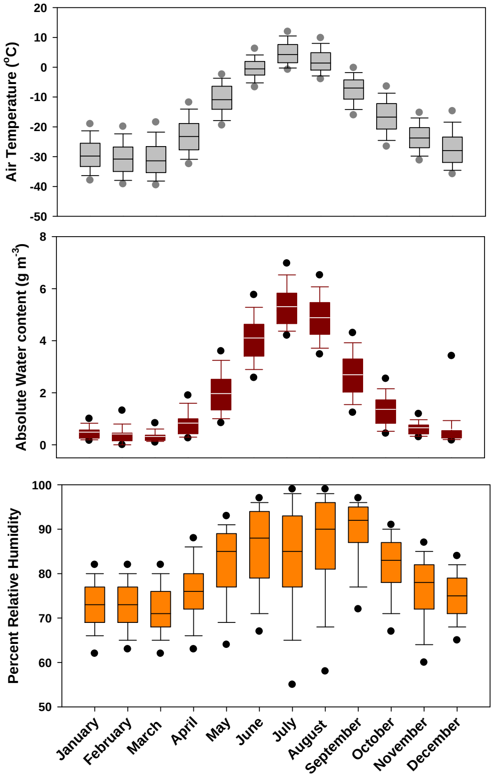

Fig. 3. Box and whisker plots of air temperature, absolute water content (AWC) and percent relative humidity (RH) data from Alert. (Air temperature and AWC are data from 2002–2011 and RH from 2004–2011). Centre line in the box represents the median value, the boundaries of the box represent the 25th and 75th percentiles, the whiskers represent the 10th and 90th percentile and the dots represent the maximum and minimum values in the data set.

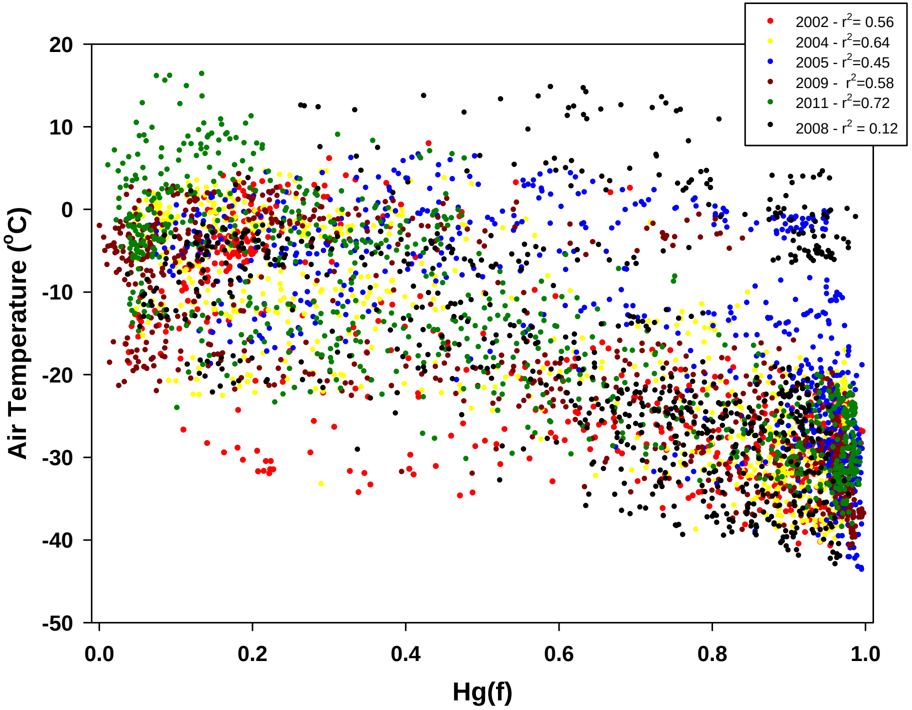

Fig. 4. Linear regression of Air Temperature versus Particulate Hg Fraction for March to June time period (Hg(f) = [PHg]/([PHg] + [RGM])). Slopes: **2002**: −27.7; **2004**: −29.4; **2005**: −29.4; **2008**: −16.5; **2009**: −26.7; **2011**: −32.4. *Years 2003, 2006, 2007 and 2010 are not included due to large data gaps.*

Title Page
Abstract | Introduction
Conclusions | References
Tables | Figures
◀| |▶
◀ ▶
Back | Close
Full Screen / Esc
Printer-friendly Version
Interactive Discussion

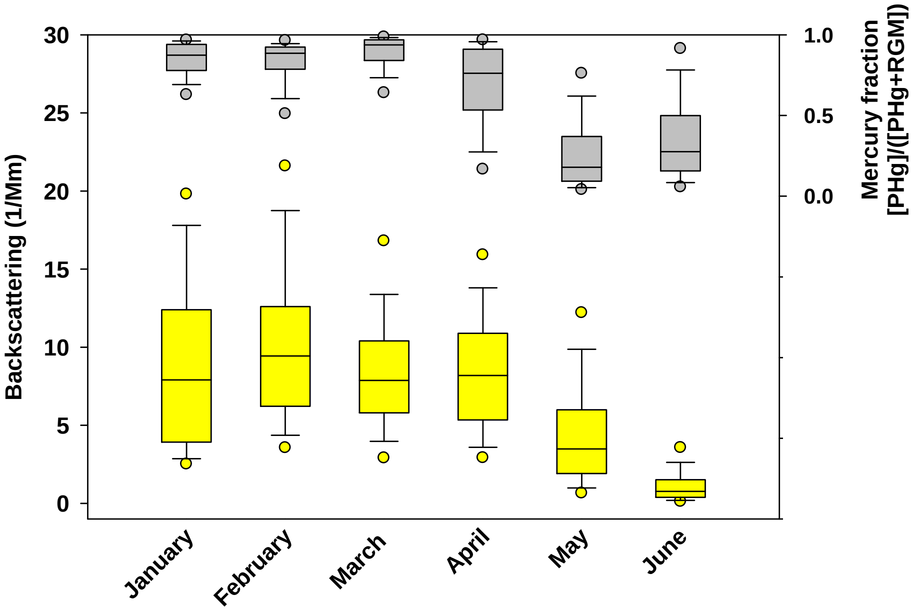

Fig. 5. Monthly box and whisker plot of backscattering (b_{sca}) and mercury fraction data from Alert. Nephelometer data is in (Mm-1) for 550 nm (yellow) from January to June 2004 to 2009. Mercury fraction data is unitless and is from January to June 2002 to 2011. Centre line in the box represents the median value, the boundaries of the box represent the 25th and 75th percentiles, the whiskers represent the 10th and 90th percentile and the dots represent the maximum and minimum values in the data set.

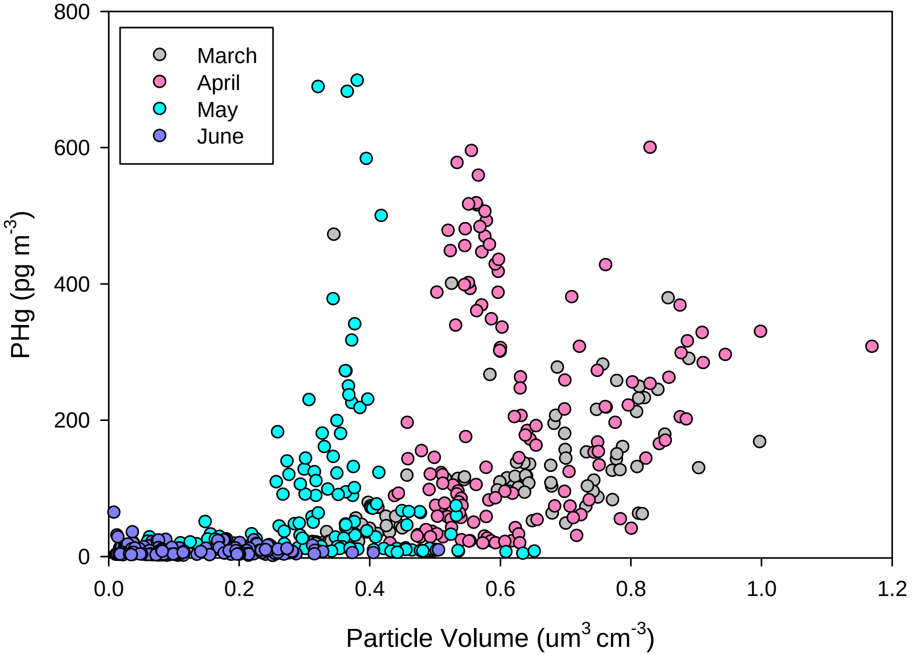

Fig. 6. Particulate mercury (PHg) concentration (pg m^{-3}) as a function of Total Volume Concentration of Particles (< 500 nm) for the months March, April, May and June 2011 at Alert, Canada.

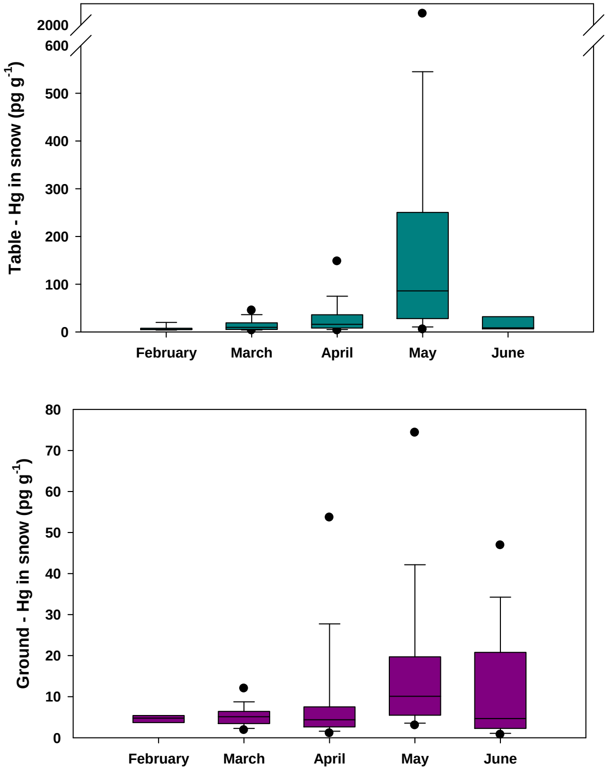

Fig. 7. Long term snow sampling measurements at Alert from 1998 to 2011 sampled on an event basis. Samples are expressed as concentration of mercury (pg g^{-1}) and were collected from a Teflon covered table (top – blue) and from the top layer of the snow pack (bottom – purple). Centre line in the box represents the median value, the boundaries of the box represent the 25th and 75th percentiles, the whiskers represent the 10th and 90th percentile and the dots represent the maximum and minimum values in the data set.

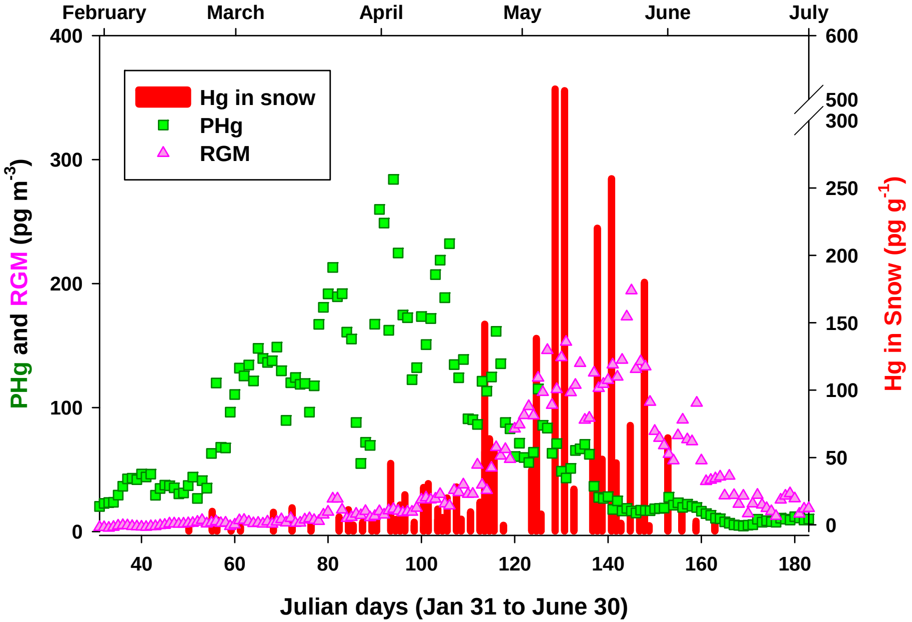

Fig. 8. Atmospheric mercury speciation concentration data PHg and RGM (pg m^{-3}) and Hg concentration (pg g^{-1}) from the snow (table) from February to June for all data from 2002 to 2011. The atmospheric data has been averaged per Julian day over all the years.